# Photovoltaic effect in micrometer-thick perovskite-type oxide multilayers on Si substrates

Hao Liu,[1,2,3] Kun Zhao,[1,2,3,a)] Na Zhou,[1,2,3] Huibin Lu,[1,b)] Meng He,[1] Yanhong Huang,[1] Kui-Juan Jin,[1] Yueliang Zhou,[1] Guozhen Yang,[1] Songqing Zhao,[2] Aijun Wang,[2] and Wenxiu Leng[2]

[1]*Beijing National Laboratory for Condensed Matter Physics, Institute of Physics, Chinese Academy of Sciences, Beijing 100080, People's Republic of China*

[2]*Department of Mathematics and Physics, China University of Petroleum, Beijing 102249, People's Republic of China*

[3]*International Center for Materials Physics, Chinese Academy of Sciences, Shenyang 110016, People's Republic of China*

(Received 26 May 2008; accepted 9 October 2008; published online 30 October 2008)

Micrometer-thick perovskite-type multilayer heterostructures with ten thousands of unit cells, $[SrNb_{0.05}Ti_{0.95}O_3/La_{0.9}Sr_{0.1}MnO_3]_3$, have been fabricated on Si substrates. The structure exhibited nonlinear and rectifying current-voltage characteristics. Stable and temporal photovoltaic effects in the multilayer have been experimentally studied by using different wavelength light sources from ultraviolet to infrared, respectively. The photovoltage and photocurrent responsivities as a function of wavelength displayed that two cutoff wavelengths occurred corresponding to the band gaps of $SrNb_{0.05}Ti_{0.95}O_3$ and Si and $La_{0.9}Sr_{0.1}MnO_3$. Under the pulsed laser illumination the nanosecond response characterization of the present multilayer structure was obtained. Based on the band structure of the multilayers, a possible mechanism of photovoltaic process was proposed. © *2008 American Institute of Physics*. [DOI: 10.1063/1.3010373]

Many techniques such as sol-gel, sputtering, pulsed laser deposition, and molecular-beam epitaxy have been used to prepare perovskite-type metal oxides, and many effects such as doping, composing and grading the films have been investigated aiming at improving the diverse properties.[1–7] Micron-sized thick perovskite-type oxide films are of great interest for applications as diverse as microwave generation and receiving, magnetic shielding, chip-to-chip interconnects, miniaturized sensors, and actuators.[8,9] Recently, Lee *et al.* announced that a three-component perovskite oxide superlattice up to 1 $\mu$m in thickness was grown on the $SrTiO_3$ substrates.[10]

Furthermore, devices such as photovoltaic and photocurrent detectors and solar cells require a certain thickness of active material in order to be sufficiently powerful/sensitive and to be of commercial interest.[11–15] So far, considerable researches have been concentrated on the photovoltaic properties of perovskite oxide thin films with typical thickness on the order of several hundred nanometers;[16–18] however, much less attention has been devoted to that of several micrometer-thick perovskite multilayer (ML) structures. In this letter, ten thousands of unit-cell (around 3 $\mu$m in thickness) perovskite-type ML heterostructures composed of Nb-doped $SrTiO_3$ and Sr-doped $LaMnO_3$ on Si substrates were fabricated, and the photovoltaic characteristics were investigated under constant and pulsed illuminations of several light sources with different wavelengths from ultraviolet to infrared.

$[SrNb_{0.05}Ti_{0.95}O_3$ (SNTO) / $La_{0.9}Sr_{0.1}MnO_3$ (LSMO)$]_3$ MLs were fabricated on *n*-Si (100) substrates (the carrier concentration: $\sim 1\times10^{16}$ cm$^{-3}$) by a computer-controlled laser molecular-beam epitaxy technique.[16] LSMO was firstly deposited on the substrate under the oxygen pressure of $3\times10^{-3}$ Pa. The second layer was SNTO whose oxygen pressure was $4\times10^{-4}$ Pa. The third and the fifth were the same as the first, and the fourth and the sixth were the same as the second. Thus, a ML structure of $[SNTO/LSMO]_3$ was created. The substrate temperature was maintained at 760 °C during deposition. For the completion of a single cell layer, 26 and 30 pulses were required for LSMO and SNTO, respectively. The structure of the sample was characterized by an *in situ* reflection high-energy electron diffraction, transmission electron microscopy (TEM), and energy dispersive spectroscopy (EDS). For the measurement for photovoltaic and transport properties, indium electrodes were placed on the surfaces of the ML and substrate, respectively. The ML/Si interface was illuminated directly (side illumination) to improve the responsivity.[17] A 632.8 nm HeNe laser (power density of 1 mW/mm$^2$), a spectrometer with selected wavelengths of 1064, 808, 532, and 355 nm, and an actively passively mode-locked Nd:YAG (yttrium aluminum garnet) laser operating at wavelengths of 1064, 532, and 355 nm with a duration of 20 ps were used to irradiate the sample at room temperature. The photovoltaic signal was monitored with a 350 MHz sampling oscilloscope terminated into 50 Ω. The photocurrent intensity was achieved by short-circuit photocurrent divided by on-sample-power, and a standard lock-in amplifier technique was employed for the short-circuit photocurrent measurement. A mixed light with a 75 W bromine tungsten lamp and a 30 W deuterium lamp was used to perform the measurement of wavelength dependence of photocurrent intensity.

Figure 1 shows a cross-sectional TEM image of $[SNTO/LSMO]_3$ ML after the mechanical polishing and Ar ion milling. The top surface appears rather rough due to damage in TEM sample preparation, and the ML thickness is fairly uniform and around 3 $\mu$m [Fig. 1(a)]. EDS analysis

a)Electronic mail: zhk@cup.edu.cn.
b)Electronic mail: hblu@aphy.iphy.ac.cn.

 

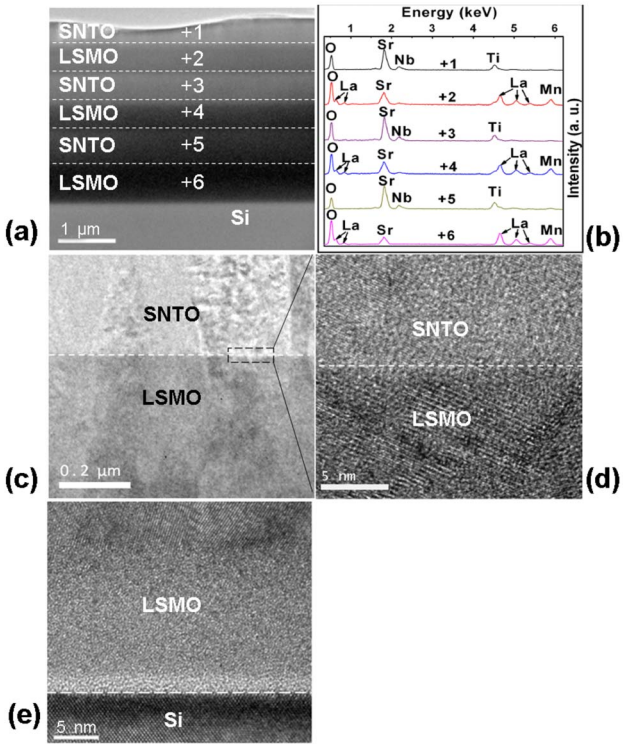


FIG. 1. (Color online) Cross-sectional TEM images of (a) $[SNTO/LSMO]_3$ ML, (c) columnar structures, (d) LSMO/Si interface, and (e) SNTO/LSMO interface. EDS analysis at selected points in (a) is shown in (b). The dashed lines denote the interface positions.

were performed at selected points, from +1 to +6, in every layer as shown in Fig. 1(b), indicating that the analyzed value are consistent with the nominal one for each layer. The microstructural characteristics are grain oriented from the interface between the ML and the Si substrate, as shown in Fig. 1(c), and these grains run through the thickness of the ML and form a columnar structure, which was also observed by Gommert *et al.*[19] and Zhou *et al.*[20] Figures 1(d) and 1(e) show the high-resolution TEM picture at LSMO/Si and SNTO/LSMO interfaces. The SNTO/LSMO interface was found to be smooth, and an amorphous interfacial layer of about 2 nm was seen at LSMO/Si interface.

The current to voltage curves at room temperature was shown in Fig. 2. At applied biases of −0.25 and 0.25 V, dark currents (DCs) of −0.021 and 0.067 mA were measured, respectively. Under an illumination of a HeNe laser, photocurrents (PCs) of −0.045 and 0.041 mA were measured at −0.25

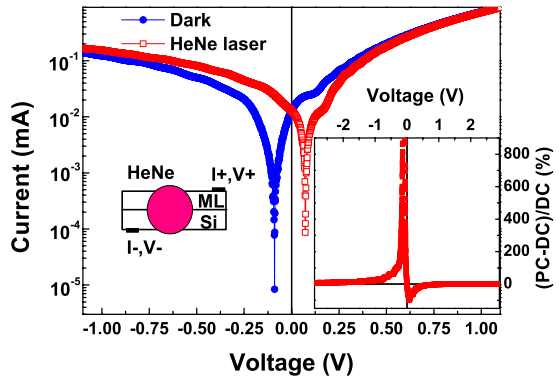


FIG. 2. (Color online) The current-voltage characteristic of the $[SNTO/LSMO]_3$ ML on Si (100) substrate under illumination (open square points) and in the dark (circle solid points) at room temperatures.

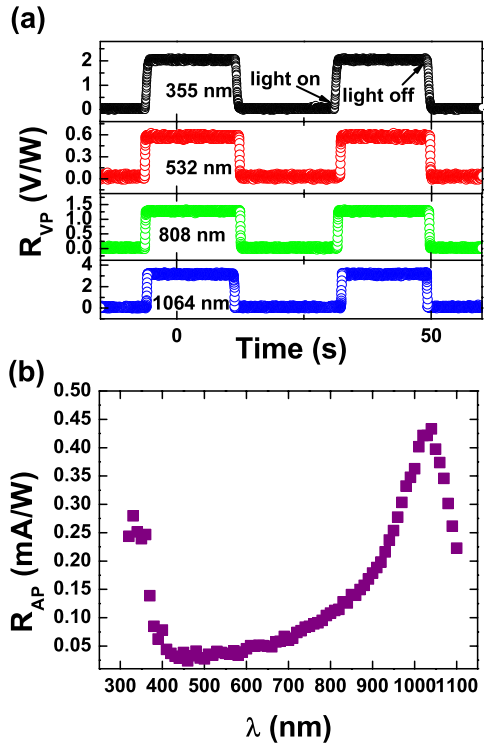


FIG. 3. (Color online) (a) Open-circuit photovoltaic sensitivity and (b) photocurrent respectivity of the $[SNTO/LSMO]_3$ ML on Si (100) substrate.

and 0.25 V. The open-circuit photovoltage and short-circuit photocurrent are 0.072 V and 0.0128 mA, respectively. It is noted that the application of a HeNe laser resulted in the decreased and increased conductivities at positive and reverse bias voltages, respectively, which is clearly shown in the inset of Fig. 2.

Figure 3(a) displays the photovoltage sensitivity $R_{VP}$, equal to photovoltage/on-sample-power, of the $[SNTO/LSMO]_3/Si$ ML under the illumination of spectrometer without an applied bias. $R_{VP}$ are about 3.15, 1.32, 0.59, and 2.06 V/W for 1064, 808, 532, and 355 nm, respectively. In addition, photocurrent responsivity $R_{AP}$, equal to short-circuit photocurrent/on-sample-power, as a function of wavelength is shown in Fig. 3(b). It can be seen that two peaks appear at ultraviolet (340 nm) and near infrared region (1040 nm). The cutoff wavelengths occur at around 440 nm and above 1100 nm, corresponding to the band gaps of SNTO (~2.8 eV), and Si (~1.12 eV), and LSMO (~1.0 eV), respectively.

The temporal response $R_{VE}$ of the MLs were measured under the illumination of Nd:YAG pulsed laser with a pulse energy density of 4.70 $\mu J/mm^2$ at room temperature as shown in Fig. 4. High-speed characterization of the present ML structure was obtained, and the rise times are about 3.86, 3.87, and 4.74 ns for 1064, 532, and 355 nm, respectively. The peak values of $R_{VE}$, $R_{VE}^P$, are 5.06, 1.47, and 1.11 V/mJ for 1064, 532, and 355 nm, respectively. $R_{VE}^P$ as a function of pulse energy densities is plotted in the inset of Fig. 4. It is found that the photovoltaic responsivity shows a high value when the sample was illuminated by low energy pulse laser and drops gradually with the increase in pulse energy density. For the intensities greater than 0.02 $mJ/mm^2$, $R_{VE}^P$ goes to saturation gradually.

Luo *et al.* described the characteristics of $La_{0.7}Ca_{0.3}MnO_3/Nb:SrTiO_3$ heterojunctions by tunneling

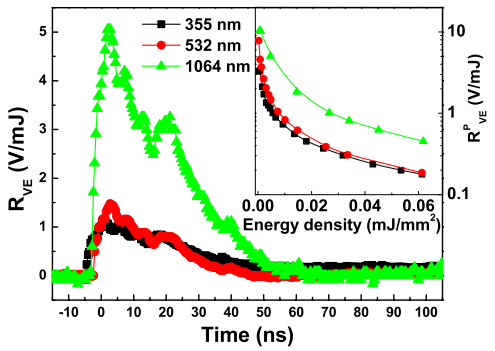


FIG. 4. (Color online) Temporal response of the $[SNTO/LSMO]_3$ MLs on Si (100) substrates under the illumination of Nd:YAG pulsed laser at room temperature without an applied bias. The inset shows the peak photovoltaic sensitivity as a function of pulse energy density.

with an effective Schottky barrier and determined the barrier height as 1.64 eV by the internal photoemission.[18] The Hall effect we measured showed that the hole concentration of the LSMO is $1.19\times10^{18}$ cm$^{-3}$, and the electron concentration of the SNTO is $1.63\times10^{20}$ cm$^{-3}$. So the $[SNTO/LSMO]_3/Si$ MLs can be treated as multi-*p*-*n* junctions, and the band structure was schematically plotted in Fig. 5 to understand the mechanism of the photovoltaic effect of the ML. The Fermi level $E_F$ of SNTO or Si is generally larger than that of manganites, when they attach, some electrons in SNTO or Si will flow into LSMO to line up the Fermi level and the same number of holes in SNTO or Si will be left. This carrier flowing causes the space charge (electron) region in LSMO and SNTO or Si (hole) near the interface. With the radiation of photons, electrons in the valence band absorbed photons and transited into the conduction band. As for the light with wavelengths above 440 nm, the photon energy is larger than the band gaps of LSMO and Si, lower than that of SNTO, so the electrons and holes in LSMO and Si were created in the system as shown in Fig. 5(a); while for the ultraviolet light, the photon energy is larger than the band gaps of LSMO, Si, and SNTO, so the electrons and holes in SNTO were also created as shown in Fig. 5(b). The created electrons with higher potential in LSMO side then flowed into the Si and SNTO sides, where the potentials were lower. Holes in Si or SNTO should move to the LSMO side by the build-in electric field in the depletion layers. Eventually, the photovoltage is produced in the forward-bias direction of the ML.

It is well known that strain due to lattice mismatch, lattice distortion due to substrate imperfection, or film thickness can strongly affect the properties of manganite thin films.[21] The present ML displays 12 times higher photovoltaic sensitivity for 1064 nm laser irradiation compared to the $La_{0.7}Sr_{0.3}MnO_3/Si$ single *p*-*n* junction where the maximum photovoltaic sensitivity was 0.435 V/mJ.[16] As seen in the TEM image [Fig. 1(e)], beyond the 2 nm initial layer on Si, the first LSMO layer experiences crystallographic disorder of about 15 nm in thickness before maintaining its crystallographic order epitaxy. This eventually reduces the effective thickness of the LSMO layer, as well as affects the photovoltage in the ML. In contrast, LSMO/SNTO interfaces were sharp without specific dislocations, as shown in Fig. 1(d). Furthermore, the LSMO layer at the LSMO/SNTO interface is expected to be in a tensile strain. Different from that induced in epitaxial single layer films, where strains get relaxed as the thickness of the film increases, strains in the case of the ML are periodically stacked. Thus the ML aspect involving a large number of LSMO/SNTO interfaces can be attributed to the enhanced photovoltaic feature.

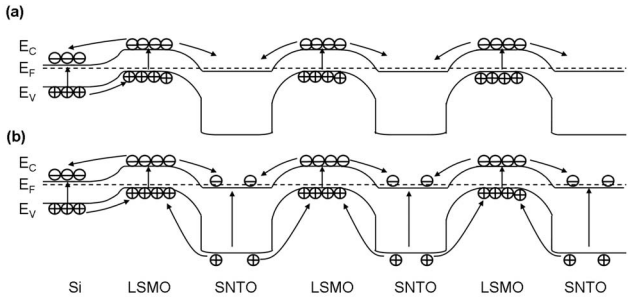


FIG. 5. The schematic band structure of the $[SNTO/LSMO]_3$ MLs on Si (100) substrates under the illuminations of (a) light with wavelengths above 440 nm and (b) ultraviolet light. $E_C$, $E_F$ and $E_V$ denoted the conduction band level, Fermi level, and valence band level, respectively.

This work has been supported by the National Basic Research Program of China, the National Natural Science Foundation of China, the Key Project of Chinese Ministry of Education, and Beijing Natural Science Foundation.

[1] R. Ranjith, R. Nikhil, and S. B. Krupanidhi, Phys. Rev. B **74**, 184104 (2006).
[2] K. Ueda, H. Tabata, and T. Kawai, Science **280**, 1064 (1998).
[3] M. P. Singh, W. Prellier, Ch. Simon, and B. Raveau, Appl. Phys. Lett. **87**, 022505 (2005); M. P. Singh, W. Prellier, L. Mechin, Ch. Simon, and B. Raveau, J. Appl. Phys. **99**, 024105 (2006); P. Murugavel and W. Prellier, J. Appl. Phys. **100**, 023520 (2006).
[4] A. R. Chaudhuri, R. Ranjith, S. B. Krupanidhi, R. V. K. Mangalam, and A. Sundaresan, Appl. Phys. Lett. **90**, 122902 (2007).
[5] S. Jin, T. H. Tiefel, M. McCormack, R. A. Fastnacht, R. Ramesh, and L. H. Chen, Science **264**, 413 (1994).
[6] H. Tanaka, J. Zhang, and T. Kawai, Phys. Rev. Lett. **88**, 027204 (2001).
[7] T. Tybell, C. H. Ahn, and J.-M. Triscone, Appl. Phys. Lett. **75**, 856 (1999).
[8] N. M. Alford, S. J. Penn, and T. W. Button, Supercond. Sci. Technol. **10**, 169 (1997).
[9] R. A. Dorey and R. W. Whatmore, J. Electroceram. **12**, 19 (2004).
[10] H. N. Lee, H. M. Christen, M. F. Chisholm, C. M. Rouleau, and D. H. Lowndes, Nature (London) **433**, 395 (2005).
[11] K.-K. Choi, B. F. Levine, C. G. Bethea, J. Walker, and R. J. Malik, Appl. Phys. Lett. **50**, 1814 (1987).
[12] K. Zweibel, H. Ullal, and B. von Roedern, Photonik Int. **10**, 48 (2004).
[13] O. Lundberg, M. Bodegård, J. Malmström, and L. Stolt, Prog. Photovoltaics **11**, 77 (2003).
[14] V. G. Karpov, M. L. C. Cooray, and D. Shvydka, Appl. Phys. Lett. **89**, 163518 (2006).
[15] A. Gupta and A. D. Compaan, Appl. Phys. Lett. **85**, 684 (2004).
[16] H. B. Lu, K. J. Jin, Y. H. Huang, M. He, K. Zhao, B. L. Chen, Z. H. Chen, Y. L. Zhou, S. Y. Dai, and G. Z. Yang, Appl. Phys. Lett. **86**, 241915 (2005); K. Zhao, Y. H. Huang, Q. L. Zhou, K. J. Jin, H. B. Lu, M. He, B. L. Cheng, Y. L. Zhou, Z. H. Chen, and G. Z. Yang, *ibid.* **86**, 221917 (2005); K. Zhao, K. J. Jin, H. B. Lu, Y. H. Huang, Q. L. Zhou, M. He, Z. H. Chen, Y. L. Zhou, and G. Z. Yang, *ibid.* **88**, 141914 (2006).
[17] J. Xing, K. Zhao, G. Z. Liu, M. He, K. J. Jin, and H. B. Lu, J. Phys. D: Appl. Phys. **40**, 5892 (2007); N. Zhou, K. Zhao, H. Liu, H. B. Lu, M. He, S. Q. Zhao, W. X. Leng, A. J. Wang, Y. H. Huang, K. J. Jin, Y. L. Zhou, and G. Z. Yang, *ibid.* **41**, 155414 (2008).
[18] Z. Luo, J. Gao, A. B. Djurišić, C. T. Yip, and G. B. Zhang, Appl. Phys. Lett. **92**, 182501 (2008).
[19] E. Gommert, H. Cerva, A. Rucki, R. v. Helmolt, J. Wecker, C. Kuhrt, and K. Samwer, J. Appl. Phys. **81**, 5496 (1997).
[20] M. J. Zhou, Y. L. Zhu, X. L. Ma, and H. B. Lu, Appl. Phys. Lett. **88**, 071905 (2006).
[21] R. A. Rao, D. Lavric, T. K. Nath, C. B. Eom, L. Wu, and F. Tsui, Appl. Phys. Lett. **73**, 3294 (1998).